Water Science & Technology

Water Science & Technology Vol 85 No 6, 1701 doi: 10.2166/wst.2022.091

Natural water defluoridation by adsorption on Laponite clay

Saber Braik[a,b], Taissire Ben Amor[b,c,*], Laure Michelin[d,e], Séverinne Rigolet[d,e], Magali Bonne[d,e], Bénédicte Lebeau[d,e] and Amor Hafiane[b,c]

[a] Research Laboratory of Environmental Science and Technologies, Borj-Cédria, 2050 Hammam-Lif, Tunisia
[b] Université de Carthage, 1054 Carthage, Tunisia
[c] Water, Membrane and Environmental Biotechnology Laboratory, CERTE, Technopole of Borj-Cedria, BP 273, Soliman 8020, Tunisia
[d] Université de Haute Alsace (UHA), CNRS, IS2M UMR 731, F-68100 Mulhouse, France
[e] Université de Strasbourg, F-67000 Strasbourg, France
*Corresponding author. E-mail: taissire.benamor@gmail.com

ABSTRACT

Safe drinking water is a necessity for every human being, but clean water is scarce and not easily available due to natural geochemical factors or industrial pollutant activity. Many issues involving water quality could be greatly improved using clays as adsorbents. We highlight for the first time, the uptake of fluoride from natural water by Laponite, synthetic hectorite clay, in raw and modified state. A series of batch adsorption experiments were carried out to evaluate the adsorption potential of the different parameters. The optimized parameters were: contact time, adsorbent dose and pH. It was found that fluoride uptake from natural water was better using raw Laponite and inorganic-modified Laponite than using organic-modified Laponite clays. Adsorbents were characterized before and after fluoride adsorption by X-ray diffraction, X-ray fluorescence, FTIR, thermo gravimetric analyses and ^{19}F solid state NMR spectroscopy. The experimental data showed that both Langmuir and Freundlich models fitted an adsorption isotherm well. Thermodynamic parameters such as Gibbs free energy ($\Delta G°$), enthalpy ($\Delta H°$), and entropy ($\Delta S°$) were calculated. These parameters indicated that fluoride adsorption onto Laponite was nonspontaneous and endothermic in temperature range between 25 and 45 °C.

Key words: adsorption, clay, fluoride removal, Laponite, water treatment

HIGHLIGHTS

- Fluoride removal from natural water by synthetic hectorite, named Laponite.
- Raw and modified Laponite have been used.
- Fluoride uptake from natural water was better using raw and inorganic-modified Laponite than using organic-modified Laponite clays.
- Both Langmuir and Freundlich models fitted an adsorption isotherm well.
- Adsorption onto Laponite was nonspontaneous and endothermic in temperature range between 25 and 45 °C.

GRAPHICAL ABSTRACT

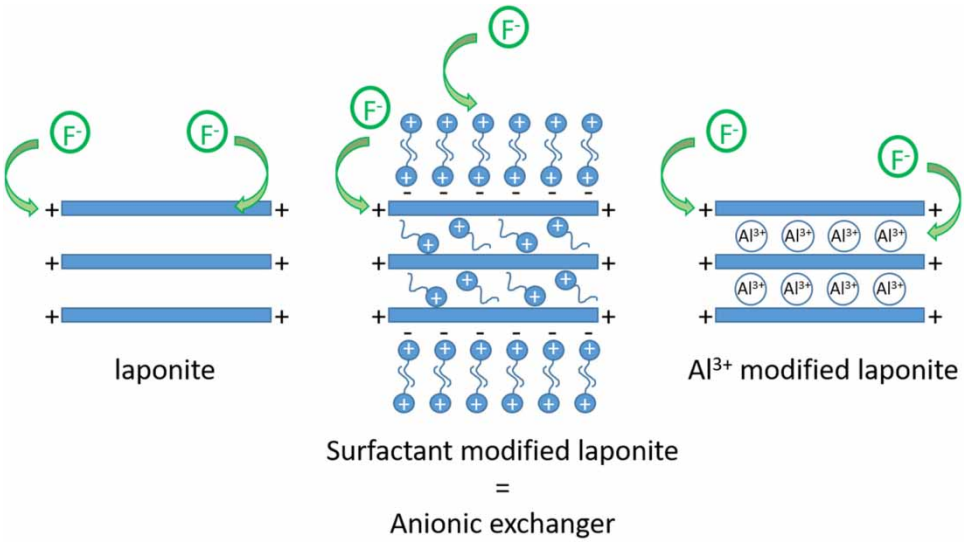

1. INTRODUCTION

Studies reveal that fluoride concentration in natural water may be way beyond the recommended limits for drinking water. The WHO guideline value for fluoride in drinking water is 1.5 $mg{\cdot}L^{-1}$ (WHO 2009). Indeed, fluoride ion is essential in human development specifically for the formation of teeth and bones if ingested at the correct concentration levels. However, too high fluoride intake causes a serious health problem affecting humans such as dental and skeletal fluorosis (Maatouk *et al.* 1998; Bhatnagar *et al.* 2011). Manifold methods are used for defluoridation of drinking water. Of all these technologies developed so far, adsorption has been considered as the most efficient and applicable technology for fluoride removal.

The adsorption process is the most attractive thanks to its effectiveness, convenience, ease of operation, and for economic and environmental reasons (Srimurali *et al.* 1998; Ramdani *et al.* 2010). Among the adsorbents tested, clays are the most widely used thanks to their large specific surface areas and chemical and mechanical stability (Ologundudu *et al.* 2016). It is expected that decrease in particle size would increase the specific surface area and offer to the solute more accessible adsorption sites (Sarkar *et al.* 2006; Maiti *et al.* 2011). In this perspective synthetic clay, such as Laponite-based nanomaterials through their mechanical, chemical and structural properties, coupled with shape, size, biodegradability and biocompatibility have gained great interest (Sabya *et al.* 2019).

Laponite is a synthetic clay mineral homologous to natural hectorite clay, which belongs to the trioctahedral smectite family. It has a distinct layered structure with permanent negative charges on basal surface and positive charges on the edges (Tawari *et al.* 2001; Ruzicka & Zaccarelli 2011).

Over the past two decades Laponite in aqueous dispersion as well as in other multicomponent systems has attracted enormous attention from academia as well as from industry. It has several applications such as being a rheology modifier and used as additive in a variety of industries such as mining, petroleum, home and personal care, pharmaceutical, agrochemical and paint polymers (Jatav & Joshi 2014). In the literature, Laponite and surface-modified Laponite have also been used for adsorption of dyes (Marandi *et al.* 2014; Mahdavinia *et al.* 2017), metals (Cao *et al.* 2018) and biomolecules (Guimaraes *et al.* 2007).

In the present study, raw and modified Laponite clays were tested for the first time, as adsorbents for defluoridation of natural water.

Fluoride could be repelled by the high density of negative charges on the basal surfaces, so natural clays could be ineffective adsorbents. There are some studies that indicate that clay minerals modified by organic surfactants become suitable materials for anion retention (Krishna *et al.* 2000; Li & Bowman 2001). The reason why is that incorporation of organic derivatives, cationic surfactants, such as $HDTMA^{+}Br^{-}$ (hexadecyltrimethyl ammonium bromide) or $HDPy^{+}Br^{-}$ (hexadecylpyridinium

bromide), onto the structure has been performed to create a new anion exchanger system and enhance anion retention capacity (Figure 1).

The surfactant bilayer could help to increase fluoride removal capacities due to change of the surface charges of the clay hybrids, which can attract and electrostatically hold anionic contaminants (Xi *et al.* 2010). The removal fluoride is mainly due to anion exchange in which the fluoride ions replace bromide ions associated with the surfactant head groups at the outer layer (Gammoudi *et al.* 2013).

Otherwise, modification of adsorbents with multivalent cations may change the surface properties of the adsorption materials and their affinity for fluoride (Guo *et al.* 2011). Documented studies reported that fluoride has strong affinity to higher density and stable electropositive polymeric species of Al^{3+}. Due to high cation exchange capacity (CEC) and surface area, clays can be modified by introducing high cationic density species such as Al^{3+} by exchange with low cationic density species such as Na^{+}, Ca^{2+}, Mg^{2+}, and K^{+} (Vhahangwela *et al.* 2014).

The main objective of the present study was to investigate the capacity of raw and modified Laponite clays in the defluoridation of natural Tunisian water. After organic ($HDTMA^{+}$ and $HDPy^{+}$) and inorganic (Al^{3+}) modification of the raw Laponite, the physicochemical characteristics of the clays were assessed. Then, the impact of parameters such as adsorbent dose, contact time and pH on the fluoride adsorption from heavily fluorinated natural water was investigated. Equilibrium adsorption isotherms, kinetic and thermodynamic study were carried out. Fluoride desorption has been also studied.

2. MATERIAL AND METHODS

2.1. Raw Laponite: Lap

Laponite is a synthetic mineral clay with chemical formula: $Na_{0.7}Si_8Mg_{5.5}Li_{0.3}O_{20}(OH)_4$. It is characterized by $pH_{PZC} = 11$ and $CEC = 0.55\ meq{\cdot}g^{-1}$. Laponite particles are disk shaped with a thickness of 1 nm and diameter of 25 ± 2 nm (Chimene *et al.* 2015).

The raw laponite image observed by scanning electron microscopy (SEM) shown in Figure 2 confirms that a Lap sample is composed of large plate-like aggregates, with irregular shape.

Laponite RD was purchased from BYK additives & Instruments. As reported in our previous work (Bippus *et al.* 2009), the specific BET surface area of Laponite RD is $351\ m^2{\cdot}g^{-1}$.

2.2. Laponite modification

2.2.1. Inorganic-modified Laponite: Lap Al

Lap Al was prepared by exchanging sodium ions (Na^{+}) with aluminum ions (Al^{3+}). Typically, 1 g of raw Laponite clay was suspended in an 100 mL aqueous solution containing $100\ mg{\cdot}L^{-1}$ of Al^{3+} prepared with $Al_2(SO_4)_3{,}18H_2O$ salt purchased from Sigma-Aldrich. After stirring for 1 h, the mixture was centrifuged at 11,000 rpm for 10 minutes to separate the solid

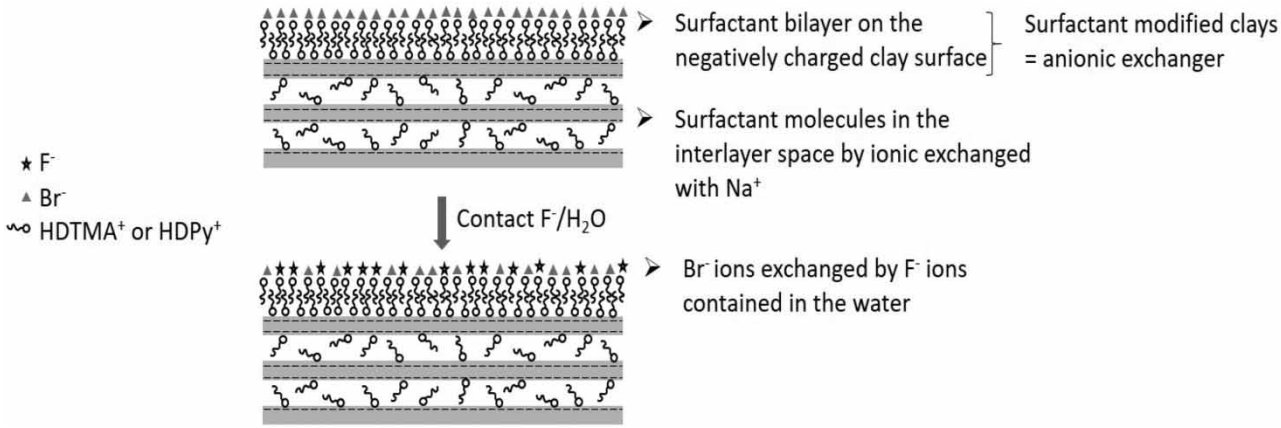

Figure 1 | Interaction between cationic surfactant ($HDTMA^{+}Br^{-}$ or $HDPy^{+}Br^{-}$) incorporated onto the Laponite clay and fluoride ions in solution.

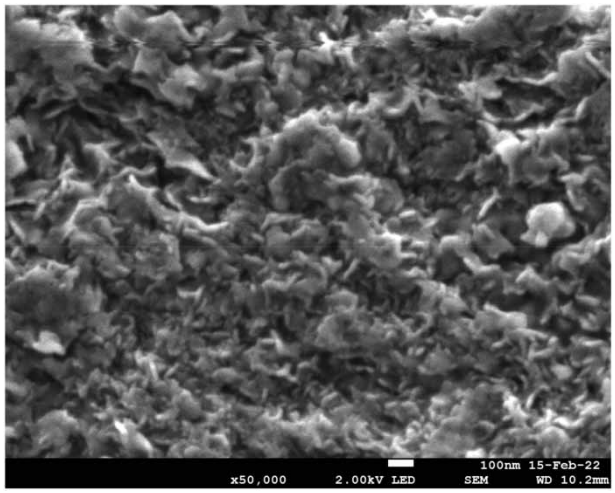

Figure 2 | Scanning electron micrographs of raw Laponite.

from supernatant. The solid phase was rinsed several times with distilled water. Finally, the solid phase was dried overnight in an oven at 60 °C.

2.2.2. Organic-modified Laponite: Lap HDTMA and Lap HDPy

Various amounts of the surfactants $HDTMA^+Br^-$ ($C_{19}H_{42}BrN$) or $HDPy^+Br^-$ ($C_{21}H_{38}BrN$) purchased from Sigma-Aldrich with initial concentrations varying from 0.5 to 3.0 CEC were dissolved in 100 mL of distilled water.

For both the $HDTMA^+$ and $HDPy^+$ surfactants, the best concentration chosen in terms of highest concentration with no or negligible surfactant crystallization was equivalent to 2.5 CEC Lap. Typically, 1 g of raw Lap was added to the surfactant solution and the mixture was stirred at 750 rpm. After stirring for 24 hours, the mixture was centrifuged at 11,000 rpm for 10 minutes to separate solid from the supernatant. The solid phase was rinsed several times with distilled water, to remove the unabsorbed surfactant molecules. Finally, the solid phase was dried in an oven at 60 °C and ground to become a powder.

2.3. Adsorbent characterization

X-ray diffraction (XRD) patterns were recorded using Cu $K_{\alpha 1\text{-}2}$ radiation ($\lambda = 0.1542$ nm) in the range $3° < 2\theta < 70°$at room temperature on an X'Pert PRO diffractometer (PANalytical).

Fourier transform infrared (FTIR) spectroscopy was used to identify the functional groups present in each adsorbent. Spectra were recorded on Bruker IFS55 spectrometer. Samples were processed at 1wt% pellets with dry KBr.

Nitrogen sorption analyses were obtained with a Micromeritics Tristar sorptometer using standard continuous procedures at 77.15 K on samples that had been degassed at 363 K for 1 h and then at 403 K under high vacuum for at least 10 h. Surface area was calculated according to the Brunauer–Emmett–Teller (BET) model over a relative pressure range of 0.05–0.30.

SEM micrographs were obtained on an JSM-7900F microscope (Tokyo, Japan). Before analysis, the samples were coated with a fine carbon layer to improve the electrical conductivity.

Wavelength dispersive X-ray fluorescence (WDXRF) was used to determine the elemental composition of adsorbents. Analyses were done using a PANalytcial Zetium spectrometer.

Thermogravimetric analyses (TGA) realized to determine the quantity of organic matter were carried out on a Mettler Toledo STARe apparatus, under air flow, with a heating rate of 5 °C·min^{-1} from 30 to 800 °C. The ^{19}FMAS NMR spectra were recorded at room temperature with a Bruker Avance II 400 MHz spectrometer operating at $B_0 = 9.4$ Tesla giving a ^{19}F Larmor frequency of 376.49 MHz, equipped with a Bruker 4 mm double channels probe. All experiments were performed at room temperature in ZrO_2 rotors, with a $\pi/2$ radio frequency pulse length of 4 μs, a recycle delay of 30 s, at a spinning rate of 12 kHz. The chemical shifts were referred to $CFCl_3$.

2.4. Optimization of fluoride adsorption conditions

The fluoride adsorption experiments were carried out in static mode at different contact times, adsorbent doses and pH. Known amounts of adsorbent were placed in polypropylene bottles containing natural fluorinated water, from Metlaoui region, Gafsa (southern of Tunisia). To investigate the effect of contact time, aliquots were collected from the solutions studied at time intervals from 30 to 180 min. The concentration of the adsorbent was varied from 5 to 20 $g{\cdot}L^{-1}$, and the initial pH of the solution was adjusted by NaOH (1M) or HCl (1M) solutions from 4 to 11. The temperature was controlled using a thermostatic bath at 25, 35 and 45 °C. After stirring, the samples were centrifuged at 11,000 rpm for 15 minutes using a centrifuge universal 320, Hettich. The fluoride ion concentration was measured with ion meter, Consort, using a combined electrode. The percentage removal of fluoride from aqueous solution was determined using the following equation:

$$[F^-](\%) = \frac{C_0 - C_e}{C_0} \times 100 \tag{1}$$

The adsorption capacity of adsorbent was computed using the following equation:

$$q = \left(\frac{C_0 - C_e}{m}\right) \times V \tag{2}$$

where C_0 is the initial fluoride concentration, C_e the equilibrium fluoride concentration ($mg{\cdot}L^{-1}$), V the volume of fluoride solution (L), and m the mass of adsorbent (g).

2.5. Modeling of analytical results

2.5.1. Adsorption isotherms

2.5.1.1. *Langmuir model.* This model is commonly used to describe the adsorption mechanism; it assumes uniform adsorption energies onto the surface. The maximum adsorption depends on the saturation level of the monolayer.

The Langmuir model can be represented with the following linear equation:

$$\frac{1}{q_e} = \frac{1}{q_m} + \frac{1}{C_e \times q_m \times b} \tag{3}$$

where q_m is the amount of adsorbate ($mg{\cdot}g^{-1}$) and b is the Langmuir isotherm constant ($L{\cdot}mg^{-1}$). The efficiency of the adsorption process can be determined with a dimensionless constant separation factor R_L, which can be calculated using the parameter b.

$$R_L = \frac{1}{1 + b \times C_0} \tag{4}$$

If the R_L values were between 0 and 1, the adsorption process is favorable for the temperature range studied.

2.5.1.2. *Freundlich model.* The Freundlich adsorption isotherm describes a heterogeneous surface energy by multilayer adsorption. This linear model is determined with the following equation:

$$\text{Log } q_e = \log K + \frac{1}{n} \log C_e \tag{5}$$

where q_e is the amount of fluoride adsorbed per unit weight of the adsorbent ($mg{\cdot}g^{-1}$), C_e is the equilibrium concentration of fluoride in the solution ($mg{\cdot}L^{-1}$), K represents the adsorption capacity, and $1/n$ is the adsorption intensity.

2.5.1.3. *Dubinin-Radushkevich (D-R).* The D-R isotherm model is used to determine the nature of the interaction between the adsorbate and the adsorbent. This helps to determine the adsorption mechanism. The D-R equation is as follow:

$$\text{Ln } q_e = \text{Ln } q_m - K_{D-R}\varepsilon^2 \tag{6}$$

where q_e is the adsorbate amount ($mol{\cdot}g^{-1}$), q_m is the maximum theoretical removal capacity ($mol{\cdot}g^{-1}$), $K_{D\text{-}R}$ is the isotherm

constant related to the adsorption energy ($mol^{-1}\cdot K^{-1}\cdot J^{-1}$), ε is the Polany potential, which is equal to RT ln $(1 + 1/C_e)$ with R and T the gas constant ($kJ\cdot mol^{-1}\cdot K^{-1}$) and K the temperature (K), respectively. C_e is the equilibrium concentration of adsorbate ($mol\cdot L^{-1}$).

2.5.2. Adsorption kinetics

2.5.2.1. *Pseudo-first-order kinetic model.* This model is used to describe the adsorption mechanism for different adsorbents. It can be written as follows:

$$\text{Ln } (q_e - q_t) = \text{Ln } q_e - k_1 t \tag{7}$$

where k_1 is the pseudo-first-order adsorption rate coefficient (min^{-1}), q_e and q_t are the values of the amount adsorbed per unit mass at equilibrium and at time t, respectively.

2.5.2.2. *Pseudo-second-order kinetic model.* This model is used to describe the adsorption process from an aqueous solution. The linearized equation of the pseudo-second-order model is given as follows:

$$\frac{t}{q_t} = \frac{1}{k_2 q_e^2} + \frac{t}{q_e} \tag{8}$$

where k_2 is the pseudo-second-order adsorption rate coefficient ($mg\cdot min^{-1}$) and q_e and q_t are the values of the amount adsorbed per unit mass at equilibrium and at time t, respectively.

2.5.2.3. *Intra-particle diffusion model.* The adsorption process may be governed by diffusional processes by the kinetics of the surface chemical reaction. The equation of the intra-particle diffusion model is given as follows:

$$q_t = k_{id} t^{1/2} + C_0 \tag{9}$$

where k_{id} is the intra-particle diffusion coefficient ($mg\cdot g^{-1}\cdot min^{-1/2}$) and C_0 is the intra-particle diffusion rate constant of the surface chemical reaction.

2.5.3. Thermodynamic modeling

The standard free energy change (ΔG°), enthalpy change (ΔH°) and entropy change (ΔS°) were calculated from the variation of equilibrium constant, K_{eq}, with temperature.

$$\Delta G^{\circ} = -\text{RTLn } K_{eq} \tag{10}$$

$$K_{eq} = \frac{C_0}{C_e} \tag{11}$$

$$\text{Ln } K_{eq} = \frac{\Delta S^0}{R} - \frac{\Delta H^0}{RT} \tag{12}$$

where R is the universal gas constant ($8.314\ J\cdot mol^{-1}\cdot K^{-1}$), T (K) is absolute temperature. Modeling of analytical results have been performed by adsorption at optimum conditions on raw and modified Laponite clays, fluoride solutions concentrations were between 10 and 100 $mg\cdot L^{-1}$ at 25, 35 and 45 °C.

3. RESULTS AND DISCUSSION

3.1. Characterization of raw and modified Laponite

XRD patterns of raw and modified Laponite clays are displayed in Figure 3(a) and 3(b).

There was no significant difference between XRD patterns of Lap and Lap Al. All the patterns of samples exhibited the widened reflections typical for disordered hectorite structure with peaks at 6.8, 19.6, 28.0, 35.0 and 60.8° (2θ), which are attributed to the (001), (110, 002), (004), (130, 200) and (060,330) crystal planes, respectively (Fischer *et al.* 2009).

For organic modified samples, XRD patterns of Lap HDTMA and Lap HDPy show that the basal spacing d(001) centered at around $2\theta° = 6.8°$ was shifted to $2\theta° = 5.6°$ and the d(004) centered at around $2\theta° = 28.0°$ was shifted to $2\theta° = 25.6°$. These

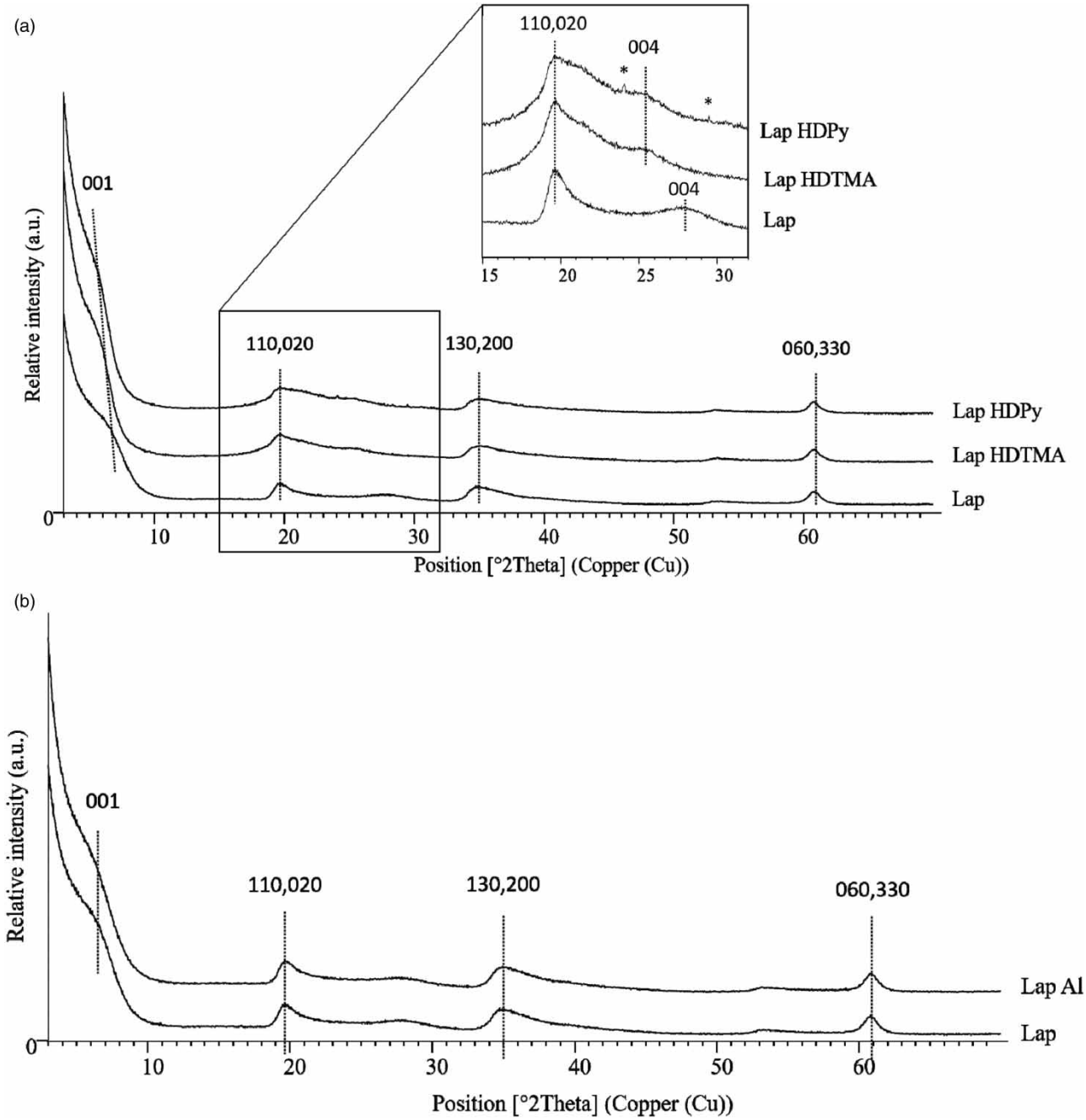

Figure 3 | XRD patterns of Lap, Lap HDTMA and Lap HDPy (a), Lap Al (b). (*correspond to $HDPy^{+}$ crystalline phase).

results indicate that surfactant cations have been intercalated within the layered structure widened the basal spacing d(001) and its harmonic d(004). At around 24.0 and 29.5°2θ low intensity peaks are also observed, which are due to the partial crystallization of the surfactant HDPy. To understand how the Laponite surface is modified, Fourier transform infrared spectroscopy (FTIR) was used for the characterization of raw and modified Laponites at a measuring range between 400 and 4,000 cm^{-1} (Figure 4).

The FTIR spectrum of the raw Lap sample presents two bands around 1,012 and 447 cm^{-1} that are attributed to Si–O stretching vibration and Si–O–Si bending mode. The band at around 662 cm^{-1} is attributed to Mg-OH bending mode. At 466 cm^{-1}, there is an overlapping of Si–O–Mg and Si–O–Si bending bands (Palkova *et al.* 2010; Zimowska *et al.* 2013).

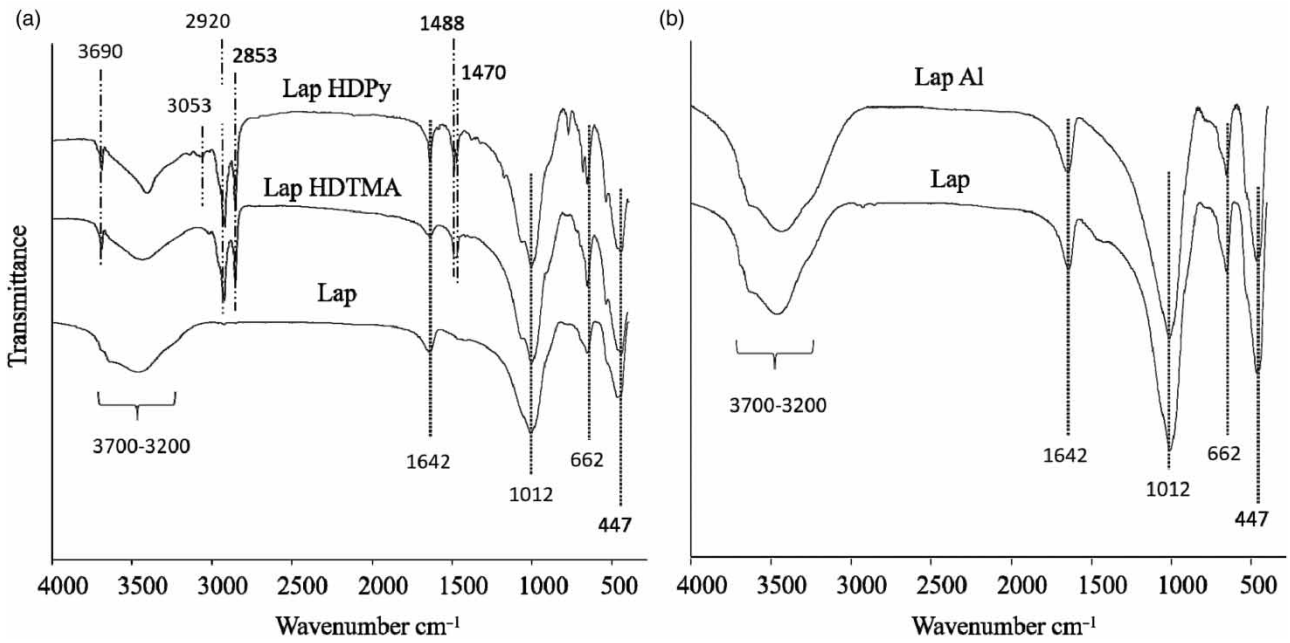

Figure 4 | FTIR spectra of Lap, Lap HDTMA and Lap HDPy (a), Lap Al (b).

The deformation vibrations of interlayer water are present at 1,642 cm^{-1}. The broad band from 3,700 to 3,200 cm^{-1} corresponded to –OH stretching vibrations of absorbed water (Xia *et al.* 2011).

A comparison of the FTIR spectra shows the appearance of new bands for the organic modified Laponite (Lap HDTMA and Lap HDPy). For Lap HDTMA, the two bands at 2,920 and 2,853 cm^{-1} correspond to the –C-H asymmetric and symmetric stretching vibrations, respectively. The bands at 1,470 and 1,488 cm^{-1} correspond to the bending vibrations of $-CH_3$ and to the CH_3 of $N(CH_3)_3$ asymmetric bending of the ammonium salt (Ologundudu *et al.* 2016; Aroke & El-Nafaty 2014). For Lap HDPy sample, the first band at 3,053 cm^{-1} is attributed to the pyridine vibration, the two bands 2,920 and 2,853 cm^{-1} are attributed to the –C-H asymmetric and symmetric stretching vibrations and the two bands at 1,470 and 1,488 cm^{-1} are attributed to the aromatic C = C vibration and aliphatic C–H stretching (Bors *et al.* 2001; Ologundudu *et al.* 2016; Aroke & El-Nafaty 2014).

The FTIR spectrum of Lap Al is very similar to the one of Lap.

The chemical composition of raw and modified Laponite was determined by XRF (Table 1).

The XRF results confirmed that raw Laponite sample is mainly composed of O, Si and Mg elements, in addition to Na. After organic modification, the presence of C, N and Br was detected in the two materials Lap HDTMA and Lap HDPy, which indicates the successful organic modification. It is noteworthy that XRF technique does not allow an accurate quantification of light elements such as C and N. Moreover, the Br/N expected to be 1 in the both Lap HDTMA and Lap HDPy materials is lower but similar (about 0.165) suggesting that most of the surfactant molecules HDTMA and HDPy have lost their Br^- counter ions following the interaction with the negatively charged surface of the Laponite. However, a decrease in sodium content is also noticed that could be attributed to the exchange of some interlayer Na^+ ions by some cationic surfactant molecules. Concerning Laponite modified with Al, an increase in Al content is clearly observed along with a decrease of Na. Thus it is assumed that some interlayer Na^+ ions have been exchanged by Al^{3+} ions.

Thermogravimetric analyses were performed on all materials before fluoride adsorption (Figure 5).

For raw Laponite material, a first weight loss of 17.5% for a temperature lower than 150 °C, was observed and attributed to dehydration of physisorbed water (Table 2). For a temperature between 150 and 800 °C a weight loss of 6.7%attributed to dehydroxylation, was noticed. In fact above 600 °C the exchangeable cations migrated into the silicate layer and the clay collapsed (Malek *et al.* 1997). The inorganic modified sample showed the same profile with a first weight loss of 9% attributed to dehydration of physisorbed water and 2% for the second weight loss attributed to dehydroxylation.

Table 1 | Elemental composition of raw and modified Laponites before and after fluoride removal from water (A) determined from by XRF analyses

	Lap		Lap A		Lap Al		Lap Al A	
Elements	**%wt[a]**	**molareq.[b]**	**%wt[a]**	**molareq.[b]**	**%wt[a]**	**molareq.[b]**	**%wt[a]**	**molareq.[b]**
O	47.8	2.99	47.7	2.98	49.5	3.09	49.1	3.07
Si	29.5	1.05	28.4	1.01	31.6	1.12	31.8	1.13
Mg	19.9	0.82	19.7	0.81	15.9	0.65	15.4	0.63
Na	2.38	0.10	1.35	0.06	0.1	0.004	0.35	0.02
Al	0.04	0.001	0.03	0.001	1.96	0.073	1.98	0.073
molar ratio								
Mg/Si		**0.78**		**0.80**		**0.58**		**0.56**
Na/Si		0.10		0.06		0.004		0.01
Al/Si		**0.001**		**0.001**		**0.065**		**0.065**
	Lap HDTMA		**Lap HDTMA A**		**Lap HDPy**		**Lap HDPy A**	
Elements	**%wt[a]**	**molareq.[b]**	**%wt[a]**	**molareq.[b]**	**%wt[a]**	**molareq.[b]**	**%wt[a]**	**molareq.[b]**
C	27.2	2.3	27.4	2.3	38.4	3.2	36.4	3.0
O	30.7	1.92	32	2.00	24.3	1.52	27.4	1.71
Si	20.4	0.73	20.3	0.72	15.9	0.57	17.3	0.62
Mg	10.9	0.45	11.4	0.47	8.7	0.36	9.57	0.39
Na	0.08	0.003	0.1	0.004	0.09	0.004	0.1	0.004
Br	4.97	0.06	1.29	0.02	5.96	0.07	2.29	0.03
Al	0.19	0.007	0.07	0.003	0.3	0.011	0.13	0.005
N	5.39	0.4	5.95	0.4	6.13	0.4	5.37	0.4
molar ratio								
Mg/Si		**0.62**		**0.65**		**0.63**		**0.64**
Br/N		**0.16**		**0.04**		**0.17**		**0.07**
N/C		0.17		0.19		0.14		0.13
Na/Si		0.005		0.006		0.007		0.007
Al/Si		0.010		0.004		0.020		0.008

[a]weight % determined by XRF.
[b]molar equivalent calculated from weight % = %wt/M with M molar weight.
Bold values indicate the most important variation in molar ratios.

For Lap HDTMA and Lap HDPy materials, in both cases, a first negligible loss of weight (<2wt%) along with endothermic phenomenon was observed from 30 to 150 °C due to the removal of physisorbed water. A multistep weight loss of about 37.6 wt% and 43.3wt% along with exothermic phenomena, which correspond to the decomposition of the organic matter corresponding to the HDTMA and HDPy, respectively, was observed from 150 to 700 °C. The small weight loss (<2wt%) from 700 to 800 °C along with exothermic phenomenon correspond to dehydroxylation of the clay sheets (Guimaraes *et al.* 2007). These TGA results are coherent with those from XRF in terms of organic matter content.

The XRD and TGA analyses clearly show that the intercalation of HDTMA and HDPy occurred by a cation exchange process. This is in agreement with the shift of d(001) and d(004) XRD peaks toward low angles due to the intercalation of the surfactant.

3.2. Optimization of adsorption parameters: contact time, adsorbent dose and initial pH of the solution

Batch experiments were carried out to evaluate the effects of contact time, adsorbent dose and pH on fluoride adsorption onto raw and modified Laponite clays.

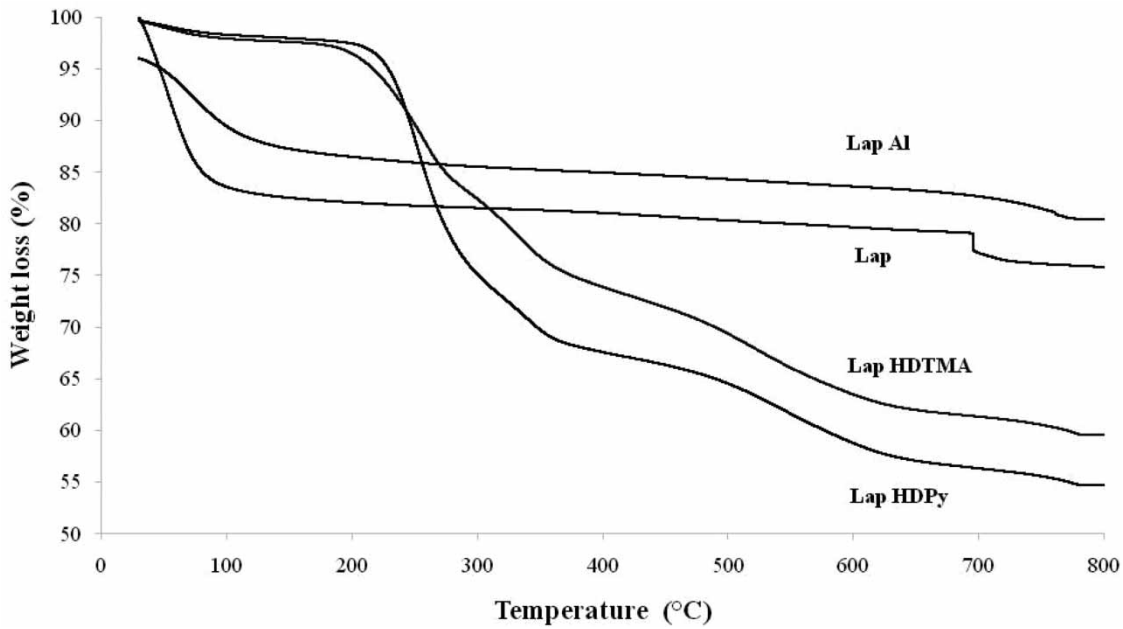

Figure 5 | TGA curves of Lap, Lap Al, Lap HDTMA and Lap HDPy.

Table 2 | Weight losses of the adsorbents determined by TG analyses

	Weight loss (%)			
Temperature ranges (°C)	Lap	Lap HDTMA	Lap HDPy	Lap Al
30 to 150	17.5	1.9	1.7	9
150 to 800	6.7	37.6	43.3	2

3.2.1. Effect of contact time

The effect of contact time on fluoride removal from natural water with raw and modified Laponite clays was studied (Figure 6(a) and 6(b)).

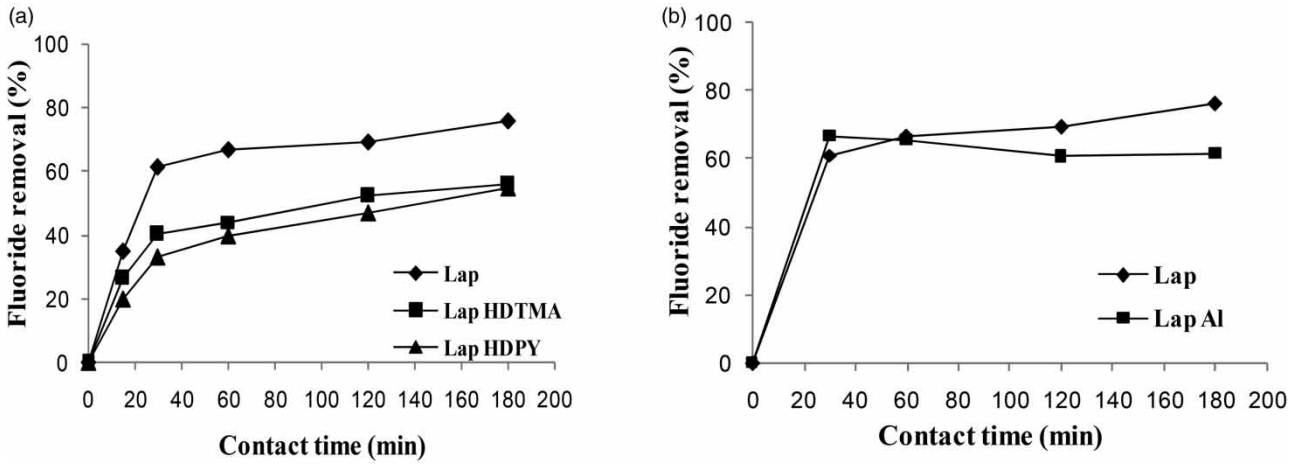

Figure 6 | Variation of fluoride removal percentage as a function of contact time for Lap, Lap HDTMA and Lap HDPy (a), Lap Al (b) ($C_0 = 3$ mg·L^{-1}; adsorbent dose = 5 g·L^{-1}; initial pH = 7; temperature = 25 °C).

The adsorption of fluoride ions onto raw and modified Laponite clay increased rapidly within the first 20 min, with equilibrium being reached at 30 min of contact time. Thereafter, no significant uptake of fluoride was observed, indicating that the reaction kinetics had reached an almost equilibrium state. On this basis, 30 min was selected as the optimum equilibrium time for further optimization experiments. The shape of the curves with a gradual increase in adsorption rather than the steep initial adsorption curve indicated that adsorption probably occur due to diffusion of fluoride ions into the pores.

The raw Laponite attains 61% and Lap Al reaches nearly 66% of fluoride removal after 30 min. However, the organically modified Lap HDTMA and Lap HDPy, respectively exhibited only 40 and 33% of fluoride removal after 30 min of contact time. Indeed, Laponite clay modification does not significantly improve the elimination rate of fluoride ions.

3.2.2. Effect of adsorbent dose

The effect of adsorbent dose on fluoride removal from natural water with raw and modified Laponite clays is shown in Figure 7(a) and 7(b).

As shown in Figure 7, fluoride removal percentage increased with an increase in adsorbent dose. The fluoride removal percentage increased rapidly from nearly 60 to 90%, as the adsorbent dose was increased from 5 to 20 $g{\cdot}L^{-1}$, respectively, for raw Laponite. Indeed, high percentage removal is attributed to more surface suitable for adsorption becoming available as the dosage increases.

For 20 $g{\cdot}L^{-1}$ as adsorbent dose, Lap Al managed to remove 94% of fluoride from the aqueous solution. However, Lap HDTMA and Lap HDPy removed only 78%.

It was concluded that 20 $g{\cdot}L^{-1}$ is the optimum adsorbent dose because it allowed us to reach values significantly lower than the standard of drinkability.

3.2.3. Effect of initial pH

The effect of initial pH on fluoride removal from natural water with raw and modified laponite clays is shown in Figure 8(a) and 8(b).

The effect of pH on fluoride removal from natural water solution was evaluated from pH 3 to 11.

A gradual decrease in fluoride removal with increase in solution pH was observed for raw and inorganic modified Laponite, this decrease is more pronounced for organic modified Laponite, which was attributed to competition of fluoride ions with excessive amount of hydroxyl ions for active sites.

The edges of Laponite particle, which contains predominantly MgOH, are positively charges below pH 11 (point of zero charge) favoring adsorption of negatively charged fluoride by electrostatic force (Ramdani *et al.* 2010; Goswami & Purkait 2011).

The highest removal efficiency was equal to 96% for Lap Al on pH lower than 7. On the basis of this, the pH of natural water (pH ≈ 6.5) was taken as the optimum pH for the subsequent experiments.

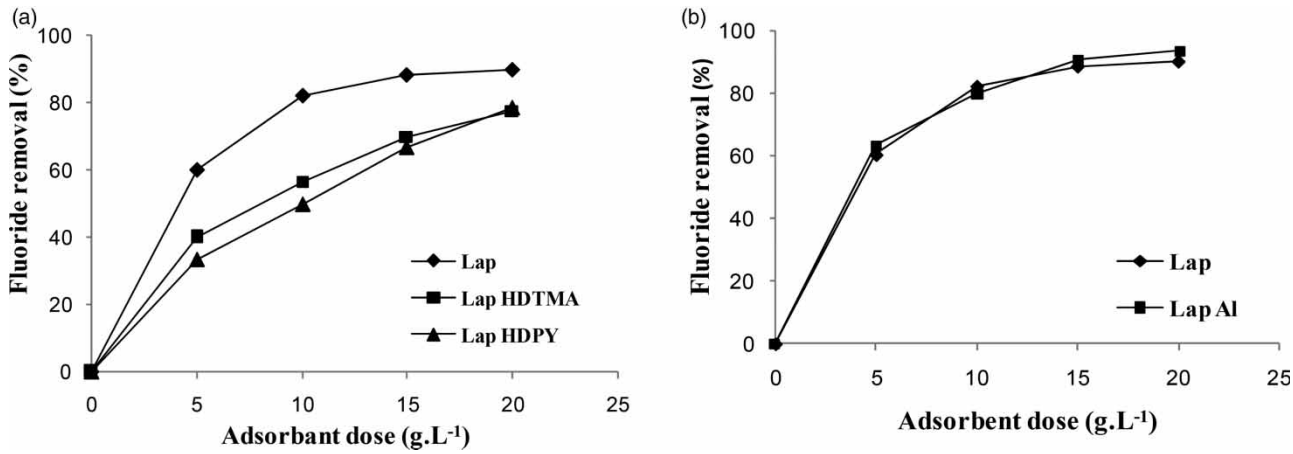

Figure 7 | Variation of fluoride removal percentage as a function of adsorbent dose for Lap, Lap HDTMA and Lap HDPy (a), Lap Al (b) ($C_0 = 3\ mg{\cdot}L^{-1}$; contact time = 30 min ; initial pH = 7; temperature = 25 °C).

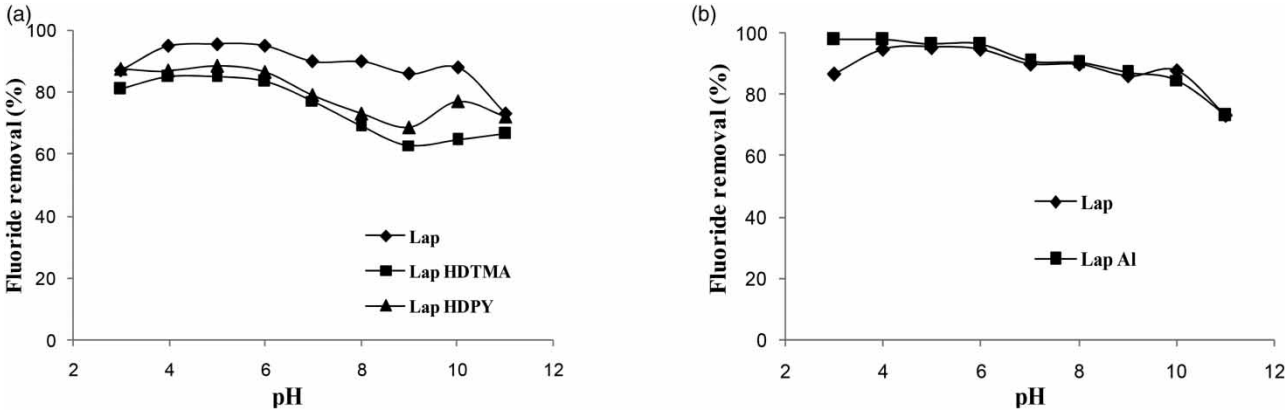

Figure 8 | Variation of fluoride removal percentage as a function of pH for Lap, Lap HDTMA and Lap HDPy (a), Lap Al (b) ($C_0 = 3$ mg·L^{-1}; contact time = 30 min ; adsorbent dose = 20 g·L^{-1}; temperature = 25 °C).

3.3. Physico-chemical characterization of water before and after treatment

Detailed physico-chemical characteristics of field water from Metlaoui city (Gafsa, southern Tunisia) before and after fluoride uptake (optimum conditions: 30 min contact time, 20 g·L^{-1} of Laponite dose, natural water pH) by the raw and modified Laponite clays were featured on Table 3.

After the contact with Laponite-based adsorbents, the fluoride-ion content decreased significantly for all clays. The best adsorption rate was obtained with Lap Al with a residual fluoride-ion content of 0.1 mg·L^{-1}.

After fluoride adsorption we noticed an increase of Na^+ and Mg^{2+} ion content accompanied with an increase of water conductivity. This is probably due to the release of these cations from the Laponite [$Na_{0.7}Si_8Mg_{5.5}Li_{0.3}O_{20}(OH)_4$] to the water. The obtained results were approved by findings of Thompson & Butterworth (1992), who have shown that for pH $\leq$ 8.5, Laponite dissolves and ions are released. Also, Mourchid & Levitz (1998) have shown that Laponite dissolution is accompanied by a release of Mg^{2+} ions, which considerably increases the ionic strength.

As indicated by some author, fluoride removal could be performed by ion exchange and the exchange was possible because of the similar ionic radii of F^- and OH^-. Waghmare and Arfin confirmed that defluoridation of water by minerals and soils could be performed with the release of OH^- ions (Waghmare & Arfin 2015). It is clear from Table 3 that pH values increases after adsorption, which confirms hydroxyl release and fluoride-ion exchange.

However, Vitani *et al.* suggested that the reactive potential of fluoride is less than the –OH decomposition energy, and thus fluoride cannot replace the –OH groups directly, particularly at low F^- concentration. Once the surface hydroxyl groups get protonated ($-OH_2^+$), the negatively charged fluorine ions are electrostatically attracted and ligand-exchange takes place (Vinati *et al.* 2015). Xiaomei *et al.* have reported that $F^-$is adsorbed on metal oxides and hydroxides through bonding interactions with the surface metal sites (Xiaomei *et al.* 2013).

Table 3 | Physico-chemical characteristics of natural water before and after treatment

		After treatment by					
Natural water	**Before treatment**	**Lap**	**Lap Al**	**Lap HDTMA**	**Lap HDPy**	**Tunisian standard**	**WHO standard**
pH	6.75	8.6	8.8	7.7	7.6	6.5–8	6.5–8
Conductivity (µS·cm^{-1})	2,900	2,850	3,400	3,250	3,300	300–2,500	–
Na^+ (mg·L^{-1})	245	–	288	329	307	200	200
K^+ (mg·L^{-1})	8.3	–	6.8	9.5	9.4	–	–
Ca^{2+} (mg·L^{-1})	229.2	96.2	167.6	212.8	224.8	300	500
Mg^{2+} (mg·L^{-1})	101.3	107	208.8	134.4	129.8	150	–
F^- (mg·L^{-1})	**3.35**	**0.20**	**0.10**	**0.50**	**0.40**	**0.8**	**1.5**

Bold values indicate the most important variation in fluoride content.

To understand the fluoride-adsorption mechanism, FTIR and ^{19}F NMR analyses were performed on raw and modified Laponite samples before and after adsorption (Figure 9).

3.4. Characterization of adsorbents after fluoride adsorption

Figure 9(a)–9(c) shows the comparison of the FTIR spectra of the raw Laponite, LapHDTMA and Lap HDPy before and after adsorption. All the spectra are very similar. Just a new peak has been seen for the Laponite HDPy at 1,384 cm^{-1}, which could correspond to aliphatic C-H stretching bonds.

The non-appearance of new bands on the FTIR spectra after fluoride adsorption indicates that fluoride removal occurred by physisorption and not chemisorption.

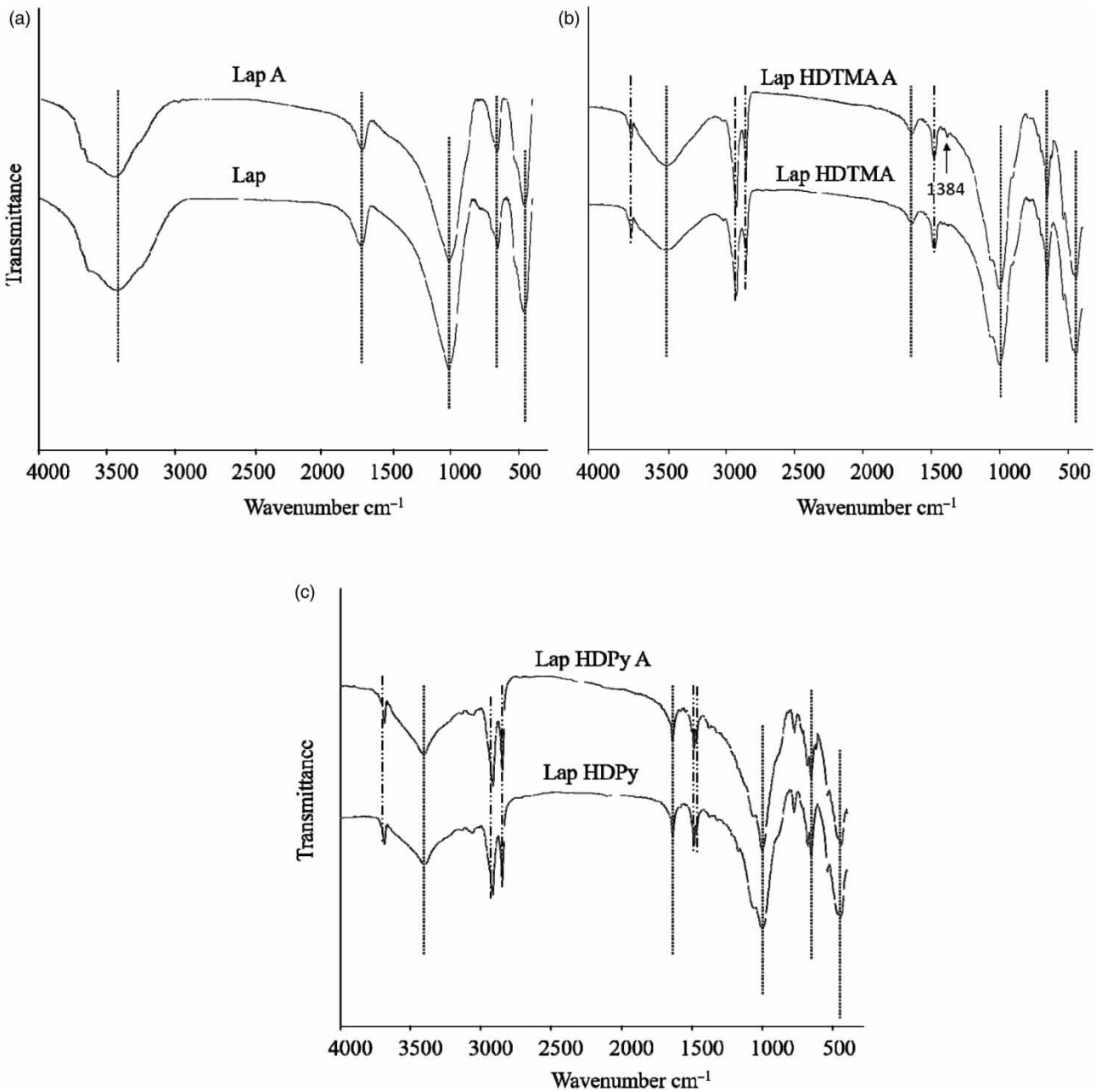

Figure 9 | FTIR spectra of Lap (a), Lap HDTMA (b) and Lap HDPy (c) before and after adsorption (Lap A, Lap HDTMA A, Lap HDPy A).

High-resolution magic-angle spinning-nuclear magnetic resonance (MAS-NMR) spectroscopy of solids is a powerful tool for understanding the fine structure of materials such as clay minerals (Huve *et al.* 1992).

It is generally agreed that substitution of hydroxyl groups by fluorine atoms occurs in clay minerals. The similarity of both their electronegativity and radius allows this substitution in most types of layer silicates.^{19}F magic-angle spinning (MAS) NMR spectroscopy was performed on raw Laponite before and after fluoride adsorption.

The ^{19}F MAS-NMR spectra of the two samples show two resonances at −182.8 and −177 ppm, indicating that two non-equivalent sites are present (Figure 10). The fluoride ions bonded to three Mg octahedral cations have a chemical shift of about -177 ppm and the resonance at −182.8 ppm in hectorite is the result of Mg substitution by Li (Huve *et al.* 1992). In the present case, the broadening and the increase of the intensity of the resonance at −177 ppm after contact with fluoride could indicate that F^- ions have substituted OH^-ions as suggested before due to the increase of water pH after fluoride adsorption (Figure 10).

For raw Laponite, no relevant changes in elemental composition were observed after contact with the fluoride-containing water (Table 1). Concerning the surfactant-modified Laponites it is interesting to note that the N/C molar ration remain constant after contact with fluoride-contained water whereas the Br/C molar ratio strongly decreased. This indicates the loss of Br as expected after exchange of Br^- by F^- ions.

3.5. Equilibrium adsorption isotherm study

The adsorption isotherm is the equilibrium relationship between the ion concentration in the aqueous solution and the solid phases (Alikhani & Moghbeli 2014). The Langmuir, Freundlich and Dubinin-Radushkevich models were used to analyze experimental data using nonlinear equations given below.

In what follows, to not clutter the manuscript with figures, only raw Laponite figures will be presented.

The equilibrium adsorption isotherms of raw Laponite at 25 °C were presented in Figure 11.

Isotherms curves in Figure 11 shows that Langmuir isotherm fits better the experimental data followed by Freundlich model.

The best isotherm was judged as the isotherm with the highest values of the regression coefficient R^2. Obtained values are given in Table 4. Both Langmuir and Freundlich models describe well the adsorption process.

The R_L values obtained (Table 4) were between 0 and 1, which indicates favorable adsorption for the temperature range studied.

3.6. Kinetic study: pseudo-first order; pseudo-second order; intra-particular diffusion

Three different types of kinetic models were used, Pseudo-first order, Pseudo-second order and Intra-particular diffusion, to investigate the adsorption kinetics of fluoride onto raw and modified Laponite (Table 5). This is to gain insight into the mechanism and rate-controlling steps affecting the kinetics of adsorption.

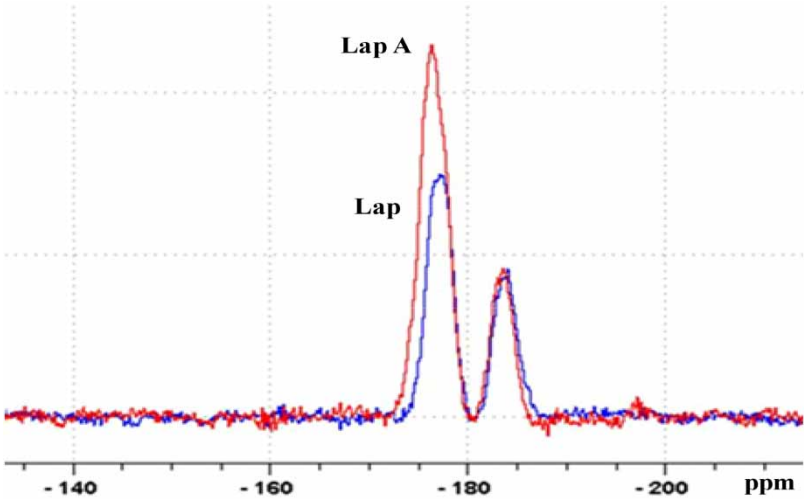

Figure 10 | ^{19}F MAS NMR spectra of Lap before and after adsorption Lap A.

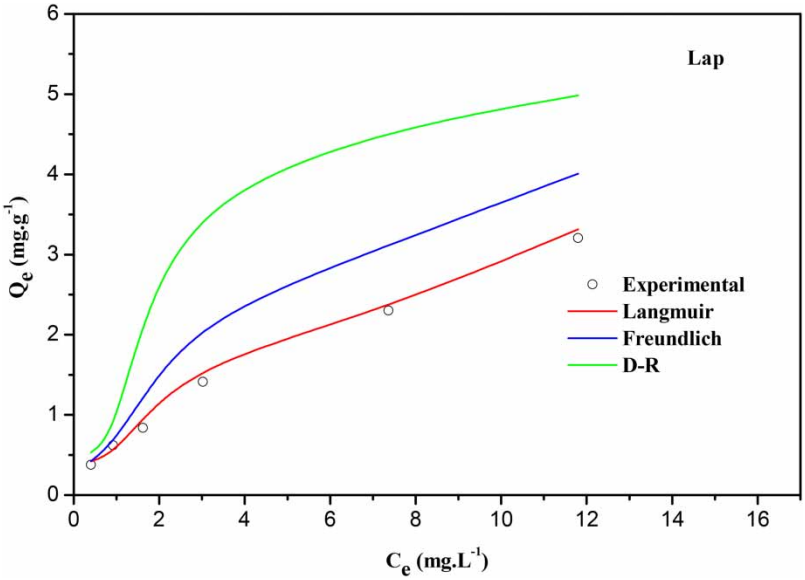

Figure 11 | Experimental data and adsorption isotherms determined by non-linear regression of fluoride ions onto Lap at 298 K.

Table 4 | Isotherm parameters

		Langmuir model			Freundlich model			D-R model		
Adsorbent	**b**	**q_m**	**R_L**	**R^2**	**K**	**n**	**R^2**	**q_m**	**E**	**R^2**
Lap	0.045	10.86	0.87	**0.983**	0.52	1.33	**0.970**	2.35	912.87	0.920
Lap Al	0.596	2.531	0.33	**0.994**	0.762	1.845	**0.991**	1.89	2,236.07	0.864
Lap HDTMA	0.004	23.35	0.98	**0.965**	0.082	0.939	**0.970**	1.64	353.55	0.657
Lap HDPy	0.015	2.958	0.95	**0.965**	0.03	0.781	**0.970**	1.21	288.67	0.740

Bold values indicate the best R^2 values.

Table 5 | Kinetic parameters

	Pseudo-first order			Pseudo-second order			Intra-particle diffusion		
Adsorbent	**k_1**	**q_e**	**R^2**	**k_2**	**q_e**	**R^2**	**k_{id}**	**C_i**	**R^2**
Lap	0.008	0.12	0.943	0.165	0.532	**0.996**	0.012	0.168	0.992
Lap Al	0.016	0.003	0.693	0.803	0.36	**0.999**	0.004	0.423	0.840
Lap HDTMA	0.016	0.158	0.986	0.191	0.356	**0.996**	0.012	0.168	0.992
Lap HDPy	0.015	0.266	0.957	0.071	0.385	**0.994**	0.022	0.029	0.949

Bold values indicate the best R^2 values.

The pseudo-second order was found to give the best fit with a correlation co-efficient of 0.996 for raw Laponite (Figure 12).

This latest model could be used to predict the kinetics of fluoride adsorption on the Laponite. The energy values found by the DR model are all less than 8,000 J·mol^{-1}, which shows that it is a physisorption (Meunier & Sun 2003). Suggesting that fluoride adsorption may be due to electrostatic attraction between the positively charged group on the adsorbent surface and negatively charged F^- at low pH.

3.7. Thermodynamic study

The curve relating Ln (Keq) to 1/T (Figure 13) allows the resolve of the thermodynamic parameters presented in Table 6.

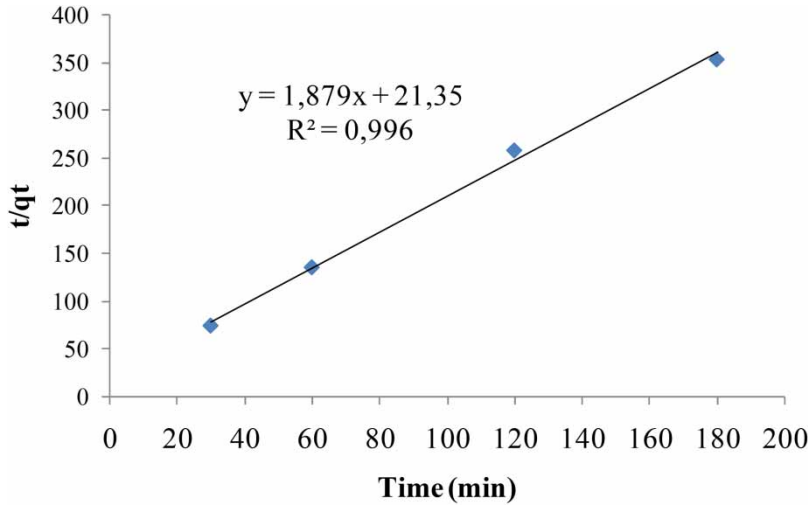

Figure 12 | Plot of pseudo-second-order model for adsorption of fluoride ions on Lap.

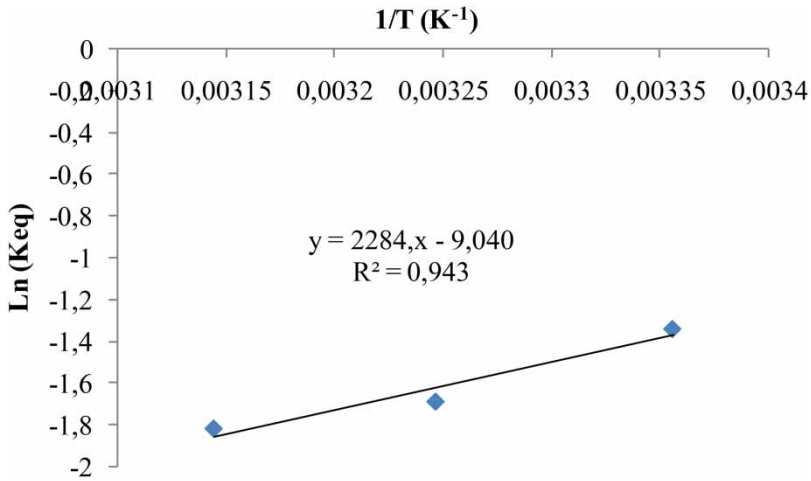

Figure 13 | Curve Ln (Keq) versus 1/T of Lap.

Table 6 | Thermodynamic parameters

Adsorbant	ΔG (J mol^{-1})			ΔH (J mol^{-1})	ΔS (J mol^{-1} K^{-1})
	298 K	308 K	318 K	298 K	298 K
Lab	41,386.4	42,138.0	42,889.6	18,989.1	−75.1
Lap Al	−21,054.6	−21,390.1	−21,725.5	−11,057.6	33.5
Lap HDTMA	5,244.9	4,939.3	4,633.8	14,349.9	30.5
Lap HDPy	5,009.2	4,697.4	4,385.6	14,300.0	31.2

In an attempt to know the behavior from a thermodynamic point of view, the raw Laponite presented a positive ΔH, which shows that the adsorption is endothermic. ΔS is negative, which suggests a non-random character at the solid-solution interface during adsorption.

For the organic modified Laponite, in both cases of Lap HDTMA and Lap HDPy, the values of ΔH are positive, therefore the adsorption is endothermic. ΔS is positive showing randomness at the solid-solution interface.

Table 7 | Adsorption capacities for the removal of fluoride by different raw clay minerals

Raw clay mineral	Adsorption capacity ($mg{\cdot}g^{-1}$)	References
Montmorillonite	1.3	Ramdani *et al.* (2010)
Pyrophyllite	2.2	Goswami & Purkait (2011)
Kaolinite	0.7	Srimurali *et al.* (1998)
Bentonite	1.2	Srimurali *et al.* (1998)
Smectite	2	Gammoudi *et al.* (2013)
Laponite	10.8	This study

For the inorganic modified Laponite Lap Al, ΔH is negative, therefore the adsorption is exothermic. ΔS is positive showing randomness at the solid-solution interface.

Results show that the standard free energy during the sorption process at 298 K were positive for raw and organic modified Laponite, which indicate that the adsorption process in the standard is non-spontaneous, and negative for the inorganic modified Laponite so the adsorption process is a favorable and spontaneous process in the standard conditions.

Table 7 gives detailed information about the adsorption capacities of fluoride by different raw clays. It is apparent from the compiled information that raw Laponite is an effective adsorbent for fluoride with higher adsorption capacity.

3.8. Desorption study on raw Laponite

Fluoride desorption from raw Laponite was tested in H_2SO_4 (2M), HCl (2M) and NaOH (2M) solutions. After the usual adsorption step, the material was placed into 13 mL of each tested solution and shaken for 1 h. The solid phase was separated from the mixture by filtration. The use of NaOH appeared to be the best choice in the striping process in terms of the recovery percentage of fluoride. Nearly 80% of fluoride adsorbed by the raw Laponite have undergone desorption process. As suggested by Thakre *et al.*, desorption of 97% was achieved using 1M NaOH solution but fluoride uptake was decreased from 95 to 73% after regeneration (Thakre *et al.* 2010).

4. CONCLUSION

In this research, the removal of fluoride ions from natural water using raw and modified Laponite clays (HDTMA, HDPy and Al) in batch experiments was investigated. The optimum conditions for fluoride removal were established as: contact time = 30 min, clay dose = 20 $g{\cdot}L^{-1}$, and natural pH water at room temperature (25 °C). Raw and inorganic modified Laponite are more efficient for removing fluoride than organic modified Laponite with an almost total elimination of fluoride ions (94 and 96%, respectively) even on heavily natural fluorinated water. An adsorption capacity of 10.8 $mg{\cdot}g^{-1}$ was determined for raw Laponite, which is much higher than raw clay's adsorption capacities studied for this purpose up to now. Adsorption isotherms revealed that the data fitted both Langmuir and Freundlich adsorption isotherms well. The pseudo-second order was found to give the best fit with a correlation co-efficiency of 99%. Standard free energy during the sorption process was positive for raw and organic modified Laponite, and negative for the inorganic modified Laponite.

ACKNOWLEDGEMENTS

Special thanks to all the staff and collaborators of the Ministry of Higher Education and Scientific Research of Tunisia the support of MESRS (Tunisia) PEJC competitive Program project 20PEJC01-13, of the Institute of Materials Science of MulhouseFrance (IS2M), specially for characterization realized on the technical ISO9001 platforms (Electron microscopy, XRD, FTIR) and of the Water Researches and Technologies Center Borj Cedria-Tunisia.

FUNDING

Taissire Ben Amor acknowledges the support of MESRS (Tunisia) PEJC competitive program project 20PEJC01-13.

CONFLICT OF INTEREST

The authors declare that they have no competing interests.

DATA AVAILABILITY STATEMENT

All relevant data are included in the paper or in its Supplementary Information.

REFERENCES

Alikhani, M. & Moghbeli, M. R. 2014 Ion-exchange polyHIPE type membrane for removing nitrate ions: preparation, characterization, kinetics and adsorption studies. *Chemical Engineering Journal* **239**, 93–104.

Aroke, U. O. & El-Nafaty, U. A. 2014 XRF, XRD and FTIR properties and characterization of HDTMA-Br surface modified organo-kaolinite. *Clay* **4**, 817.

Bhatnagar, A., Kumar, E., Kumar, U. & Sillanpaa, M. 2011 Defluoridation from aqueous solutions by Nano-Aluminsa: characterization and sorption studies. *Journal of Hazardous Materials* **186**, 1042–1049.

Bippus, L., Jaber, M. & Lebeau, B. 2009 Laponite and hybrid surfactant/laponite particles processed as spheres by spray-drying. *New Journal of Chemistry* **33**, 1116–1126.

Bors, J., Patzko, A. & Dekany, I. 2001 Adsorption behavior of radio iodides in hexadecyl– pyridinium–humate complexes. *Applied Clays Science V* **19** (1), 27–37.

Cao, X., Yan, B., Huang, Y., Zhang, Y., Li, L., Qiu, J. & Lyu, X. 2018 Use of Laponite as adsorbents for Ni(II) removal from aqueous solution. *Environmental Progress & Sustainable Energy* **37**, 942–950.

Chimene, D., Alge, D. L. & Gaharwar, A. K. 2015 Two-dimensional nanomaterials for biomedical applications: emerging trends and future prospects. *Advanced Materials* **27**, 7261–7284.

Fischer, H., Weidler, P. G., Grobety, B., Luster, J. & Gehring, A. U. 2009 The transformation of synthetic hectorite in the presence of Cu(II). *Clays and Clay Minerals* **57** (2), 139–149.

Gammoudi, S., Frini-Srasra, N. & Srasra, E. 2013 Preparation, characterization of organosmectites and fluoride ion removal. *International Journal of Mineral Processing* **125**, 10–17.

Goswami, A. & Purkait, M. K. 2011 Kinetic and equilibrium study for the fluoride adsorption using pyrophyllite. *Separation Science & Technology* **46**, 1797–1807.

Guimaraes, A. M. F., Ciminelli, V. S. T. & Vasconcelos, W. L. 2007 Surface modification of synthetic clay aimed at biomolecule adsorption: synthesis and characterization. *Journal of Materials Research* **10**, 37–41.

Guo, H., Li, W., Chang, Z., Wang, H. & Zhou, Y. 2011 Mechanism study of fluoride adsorption by hydrous metal oxides. *Spectroscopy & Spectral Analysis* **31**, 2210–2214.

Huve, L., Delmotte, L., Martin, P., Le Dred, R., Baron, J. & Saehr, D. 1992 ^{19}F MAS-NMR study of structural fluorine in some natural and synthetic 2:1 layer silicates. *Clays and Clay Minerals* **40**, 186–191.

Jatav, S. & Joshi, Y. M. 2014 Chemical stability of Laponite in aqueous media. *Applied Clay Science* **97**, 72–77.

Krishna, B. S., Murty, D. S. R. & Prakash, B. S. J. 2000 Thermodynamics of chromium (VI) anionic species sorption onto surfactant-modified montmorillonite clay. *Journal of Colloid and Interface Science* **229** (1), 230–236.

Li, Z. & Bowman, R. S. 2001 Retention of inorganic oxyanions by organo-kaolinite. *Water Research* **35** (16), 3771–3776.

Maatouk, F., Ameur, A., Ghedira, H., Belgacem, B. & Bourgeois, D. 1998 School oral health survey in Kairouan,Tunisia. *Eastern Mediterranean Health Journal* **4**, 137–141.

Mahdavinia, G. R., Soleymani, M., Sabzi, M., Azimi, H. & Atlasi, Z. 2017 Novel magnetic polyvinyl alcohol/laponite RD nanocomposite hydrogels for efficient removal of methylene blue. *Environnmental Chemical Engineering* **5**, 2617–2630.

Maiti, A., Basu, J. K. & De, S. 2011 Chemical treated laterite as promising fluoride adsorbent for aqueous system and kinetic modeling. *Desalination* **265**, 28–36.

Malek, Z., Balek, V., Garfinkel-Shweky, D. & Yariv, S. 1997 The study of the dehydration and dehydroxylation of smectites by thermal analysis. *Journal of Thermal Analysis and Calorimetry* **48**, 83–92.

Marandi, G. B., Baharloui, M., Kurdtabar, M., Mahmoodpoor, L. & Sharabian, M. A. 2014 Hydrogel with high laponite content as nanoclay: swelling and cationic dye adsorption properties. *Research on Chemical Intermediates* **41**, 7043–7058.

Meunier, F. & Sun, L. M. 2003 Adsorption – Aspects théoriques Tech. Techniques de l'ingénieur Procédés de traitement des eaux potables, industrielles et urbaines, base documentaire. TIB318DUO

Mourchid, A. & Levitz, P. 1998 Long-termgelation of laponite aqueous dispersions. *Physical Review E* **57** (5), 4887–4890.

Ologundudu, T. O., Odiyo, J. O. & Ekosse, J. O. I. 2016 Fluoride sorption efficiency of vermiculite functionalised with cationic surfactant: isotherm and kinetics. *Applied Science* **6**, 1–15.

Palkova, P., Madejova, J., Zimowska, M. & Serwicka, E. M. 2010 Laponite-derived porous clay heterostructures: II. FTIR study of the structure evolution. *Microporous and Mesoporous Materials* **127**, 237–244.

Ramdani, A., Taleb, S., Benghalem, A. & Ghaffour, N. 2010 Removal of excess fluoride ions from Saharanbrackish water by adsorption on natural materials. *Desalination* **250**, 408–413.

Ruzicka, B. & Zaccarelli, E. 2011 A fresh look at the Laponite phase diagram. *Soft Matter* **7**, 1268–1286.

Sabya, S. D., Neelam, K. H., Sima, S., Afzal, H., Abdul, F. & Mike, T. 2019 Laponite-based nanomaterials for biomedical applications: a review. *Current Pharmaceutical Design* **25**, 424–443.

Sarkar, M., Banerjee, A. & Pramanick, P. P. 2006 Kinetics and mechanism of fluoride removal using laterite. *Industrial & Engineering Chemistry Research* **45**, 5920–5927.

Srimurali, M., Pragathi, A. & Karthikeyan, J. 1998 A study on removal of fluorides from drinking water by adsorption onto low-cost materials. *Environmental Pollution* **99**, 285–289.

Tawari, S. L., Koch, D. L. & Cohen, C. 2001 Electrical double-layer effects on the brownian diffusivity and aggregation rate of laponite clay particles. *Journal of Colloids and Interface Science* **240**, 54–66.

Thakre, D., Rayalu, S., Kawade, R., Meshram, S., Subrt, J. & Labhsetwar, N. 2010 Magnesium incorporated bentonite clay for defluoridation of drinking water. *Journal of Hazardous Materials* **180**, 122–130.

Thompson, D. W. & Butterworth, J. T. 1992 The nature of laponite and its aqueous dispersions. *Journal of Colloid and Interface Science* **151** (1), 236–243.

Vhahangwele, M., Mugera, G. W. & Tholiso, N. 2014 Defluoridation of drinking water using Al^{3+} modified bentonite clay: optimization of fluoride adsorption conditions. *Toxicology and Environmental Chemistry* **96**, 1294–1309.

Vinati, A., Mahanty, B. & Behera, S. K. 2015 Clay and clay minerals for fluoride removal from water: a state-of-the-art review. *Applied Clay Science* **114**, 340–348.

Waghmare, S. S. & Arfin, T. 2015 Fluoride removal by clays, geomaterials, minerals, low cost materials and zeolites by adsorption: a review. *International Journal of Science, Engineering and Technology Research* **4**, 3663–3676.

WHO 2009 *International Standards for Drinking Water*. World Health Organisation, Geneva.

Xi, Y., Mallavarapu, M. & Naidu, R. 2010 Preparation, characterization of surfactants modified clay minerals and nitrate adsorption. *Applied Clay Science* **48**, 92–96.

Xia, C., Jing, Y., Jia, Y., Yue, D., Ma, J. & Yin, X. 2011 Adsorption properties of Congo red from aqueous solution on modified hectorite: kinetic and thermodynamic studies. *Desalination* **265**, 81–87.

Xiaomei, W., Zhang, Y., Xiaomin, D., Bei, Z. & Yang, M. 2013 Fluoride adsorption on an Fe–Al–Cetrimetal hydrous oxide: characterization of adsorption sites and adsorbed fluorine complex species. *Chemical Engeneering Journal* **223**, 364–370.

Zimowska, M., Pálková, L., Madejová, J., Dula, R., Pamin, K., Olejniczak, Z., Gil, B. & Serwicka, E. M. 2013 Laponite-derived porous clay heterostructures: III. The effect of alumination. *Micropor ous and Mesoporous Materials* **175**, 67–75.

First received 20 January 2022; accepted in revised form 3 March 2022. Available online 16 March 2022